STATISTICS, OPTIMIZATION AND INFORMATION COMPUTING
Stat., Optim. Inf. Comput., Vol. **x**, Month 202x, pp 0–20.
Published online in International Academic Press (www.IAPress.org)

Statistical Analysis of Saudi Arabia's Environmental Indicator using Log-Logistic Current Records

Mahmoud Magdy Barbary[1], Ramy Abdelhamid Aldallal[2,*]

[1]Department of Finance, College of Business Administration in Hawtat Bani Tamim, Prince Sattam bin Abdulaziz University, Hawtat Bani Tamim, Saudi Arabia.
[2]Department of Management, College of Business Administration in Hawtat Bani Tamim, Prince Sattam bin Abdulaziz University, Hawtat Bani Tamim, Saudi Arabia.

Abstract Accurate modeling and prediction of atmospheric pressure are essential for climate monitoring, weather forecasting, and environmental sustainability planning. Motivated by the importance of analyzing atmospheric-pressure variability in Riyadh, Saudi Arabia, this paper develops a comprehensive statistical framework for upper and lower current records under the Log-Logistic distribution. New closed-form probability density and cumulative distribution functions are derived using recently established general current-record formulas. Joint and conditional density functions, moments, Shannon entropy, and extropy are also obtained. Maximum likelihood and Bayesian methods are proposed to estimate the unknown parameters, while Bayesian posterior predictive procedures are developed to predict future current records. Since the resulting likelihood equations have no closed-form solutions, numerical optimization and Markov Chain Monte Carlo algorithms are employed for estimation and prediction. A Monte Carlo simulation study demonstrates that estimation accuracy improves as the number of current records increases, with the Bayesian approach providing slightly more stable estimates. The proposed methodology is applied to daily atmospheric-pressure observations from Riyadh, where the Log-Logistic distribution provides an excellent fit and yields reliable predictions of future pressure extremes. The proposed framework offers an effective statistical tool for modeling and predicting sequential atmospheric-pressure extremes and may support meteorological monitoring and environmental risk assessment.

Keywords Bayesian prediction; Estimation; Entropy and Extropy; Log-Logistic current records; Saudi Arabia Atmospheric pressure data;

AMS 2010 subject classifications 62F15, 62G32, 62P12

DOI: 10.19139/soic-2310-5070-4351

1. Introduction

Climate change has become one of the most important environmental challenges facing countries worldwide. Changes in temperature, precipitation, wind patterns, humidity, and atmospheric pressure can influence natural ecosystems, water resources, agricultural productivity, human health, and the frequency of extreme weather events.

Atmospheric pressure is a fundamental meteorological variable that plays a key role in the movement of air masses, wind circulation, cloud formation, rainfall, and the development of different weather conditions. Variations in atmospheric pressure also influence aviation, transportation, agriculture, air quality, and public health. Consequently, accurate monitoring and statistical analysis of atmospheric-pressure measurements provide valuable

*Correspondence to: Ramy Abdelhamid Aldallal (Email: dr.raldallal@gmail.com). Department of Management, College of Business Administration in Hawtat Bani Tamim, Prince Sattam bin Abdulaziz University, Hawtat Bani Tamim, Saudi Arabia.

ISSN 2310-5070 (online) ISSN 2311-004X (print)

insights into short-term weather variability, long-term regional climate changes, and unusual environmental conditions [15].

The study of atmospheric pressure is particularly relevant in Saudi Arabia because of the Kingdom's arid climate, large desert areas, high temperatures, limited rainfall, and frequent dust and sand storms. Variations in pressure may contribute to changes in wind speed, visibility, and weather stability, making pressure monitoring important for environmental management and operational planning.

Saudi Arabia has shown increasing interest in climate monitoring and environmental sustainability through Saudi Vision 2030 and the Saudi Green Initiative. These programs emphasize environmental protection, emission reduction, sustainable resource management, and the development of reliable systems for observing climate-related indicators [12, 16]. Statistical modeling of atmospheric variables can support these national objectives by providing useful information for forecasting, risk assessment, and evidence-based environmental planning.

Motivated by the importance of atmospheric monitoring, this paper analyzes atmospheric-pressure measurements recorded in Riyadh, Saudi Arabia. The study develops estimation and Bayesian prediction procedures for upper and lower current records under the Log-Logistic distribution. The proposed methods are evaluated through Monte Carlo simulation and then applied to real atmospheric-pressure data.

The Log-Logistic distribution is a flexible two-parameter continuous distribution defined on the positive real line. It is characterized by a positive scale parameter $\alpha > 0$ and a positive shape parameter $\beta > 0$. Its cumulative distribution function is

$$F(x;\alpha,\beta) = \frac{1}{1+(x/\alpha)^{-\beta}} = \frac{x^{\beta}}{\alpha^{\beta}+x^{\beta}}, \qquad x > 0, \tag{1}$$

while its probability density function is

$$f(x;\alpha,\beta) = \frac{\beta}{\alpha}\frac{(x/\alpha)^{\beta-1}}{\left[1+(x/\alpha)^{\beta}\right]^2} = \frac{\beta\alpha^{\beta}x^{\beta-1}}{\left(\alpha^{\beta}+x^{\beta}\right)^2}, \qquad x > 0. \tag{2}$$

The corresponding survival function is

$$\overline{F}(x;\alpha,\beta) = 1 - F(x;\alpha,\beta) = \frac{1}{1+(x/\alpha)^{\beta}}. \tag{3}$$

The Log-Logistic distribution is suitable for positive and skewed environmental data because it has simple closed-form expressions for its distribution, density, survival, and quantile functions. The parameter α controls the scale of the distribution, whereas β determines its shape and tail behavior. These properties make it a useful model for atmospheric-pressure observations.

The concept of current records arises from the statistical analysis of sequential extreme observations. Houchens [13] established important distributional properties of current records and provided a foundation for inference based on this type of data. Barakat et al. [10, 11] studied current records, record ranges, and exact prediction intervals, while Raqab [17, 19, 18] developed several inequalities and distribution-free prediction procedures. More recently, Aldallal and co-authors proposed estimation, Bayesian inference, and prediction methods for current records under different probability distributions and illustrated their applications to real data [2, 5, 1, 4, 6, 3, 7, 9]. A broader review of the classical and recent developments in current-record theory is presented by Aldallal and Barakat [8].

1.1. Current records and their interpretation

For clarity, it is useful to distinguish current records from the usual record values. In a sequence of observations $X_1, X_2, \ldots$, an ordinary upper record value is observed whenever a new observation exceeds all previously observed values, whereas an ordinary lower record value occurs whenever a new observation is smaller than all previous observations. Thus, the ordinary upper and lower record sequences contain only the observations at which new extremes are established.

Current records, in contrast, describe the pair of extreme values that are currently in force whenever either a new upper or a new lower record occurs. Consequently, when a new lower record is observed, the current lower record is updated while the current upper record remains equal to its most recently established value. Similarly, when a new upper record occurs, the upper current record is updated while the lower current record remains unchanged. Therefore, current records retain information about the simultaneous evolution of the upper and lower extremes of the observed process.

For example, consider the sequence

$$10,\ 8,\ 7,\ 9,\ 12,\ 11,\ 6.$$

Starting from the first observation, the successive pairs of upper and lower current records are

$$(10,10),\quad (10,8),\quad (10,7),\quad (12,7),\quad (12,6).$$

The observation 9 does not generate a new current-record pair because it is neither larger than the current upper record 10 nor smaller than the current lower record 7. Likewise, the observation 11 does not establish a new record after the upper record has become 12. This simple example illustrates how current records preserve the currently active upper and lower extremes rather than considering the two ordinary record sequences separately.

Since the Log-Logistic distribution considered in this paper is absolutely continuous, ties occur with probability zero theoretically. In an empirical dataset, if equal observations occur because of measurement rounding, an observation equal to the existing maximum or minimum is not treated as a new record; the corresponding current record simply remains unchanged.

2. PDF and CDF of current records

In this section, explicit probability density functions (PDFs) and cumulative distribution functions (CDFs) are derived for the upper and lower current records associated with the Log-Logistic distribution. By substituting the Log-Logistic distribution and density functions into the general current-record formulas established by [1], closed-form expressions for the proposed current-record distributions are obtained. These results provide the theoretical foundation for the estimation, simulation, and Bayesian prediction procedures developed in the subsequent sections.

Theorem 1
From the new current records formulas founded by [1] and using equations (1), (2), and (3), we get the PDF and CDF of Log-Logistic upper and lower current records as follows

$$F_{L^p_{\tilde{c}r}}(x) = 1 + \frac{2^p}{1+(x/\alpha)^{-\beta}} G\left(p, \log(1+(x/\alpha)^{-\beta})\right) - G\left(p, 2\log(1+(x/\alpha)^{-\beta})\right), \tag{4}$$

$$f_{L^p_{\tilde{c}r}}(x) = \frac{2^p \beta (x/\alpha)^{\beta-1}}{\alpha(1+(x/\alpha)^{\beta})^2} G\left(p, \log(1+(x/\alpha)^{-\beta})\right), \tag{5}$$

$$F_{U^p_{\tilde{c}r}}(x) = G\left(p, 2\log(1+(x/\alpha)^{\beta})\right) - \frac{2^p}{1+(x/\alpha)^{\beta}} G\left(p, \log(1+(x/\alpha)^{\beta})\right), \tag{6}$$

$$f_{U^p_{\tilde{c}r}}(x) = \frac{2^p \beta (x/\alpha)^{\beta-1}}{\alpha(1+(x/\alpha)^{\beta})^2} G\left(p, \log(1+(x/\alpha)^{\beta})\right). \tag{7}$$

Figures 1–3 illustrate the probability density functions (PDFs) and cumulative distribution functions (CDFs) of the proposed upper and lower current-record distributions for different values of the record number p under several combinations of the Log-Logistic parameters (α, β). It is evident that all CDFs are monotone increasing and converge to one as x increases, confirming the validity of the newly derived distributions.

For the lower current records, the CDFs become steeper as the record number p increases, indicating that successive lower current records become increasingly concentrated. The corresponding PDFs exhibit unimodal shapes, with their modes shifting slightly toward larger values of x while becoming more peaked, reflecting a gradual reduction in variability.

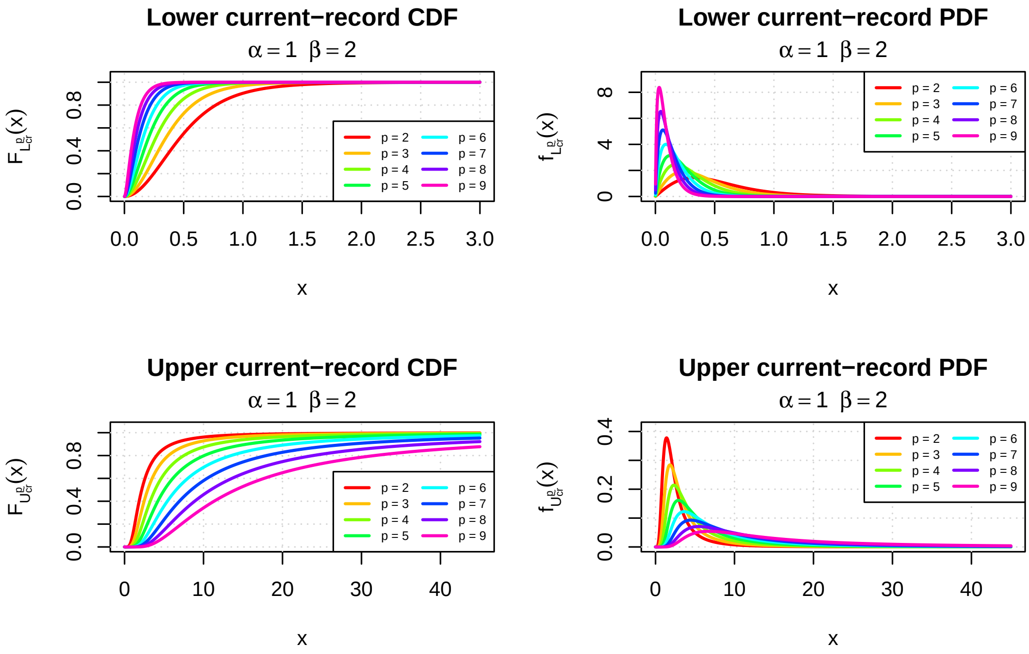

Figure 1. PDF and CDF of upper and lower current records for $\hat{\alpha} = 1$ and $\hat{\beta} = 2$.

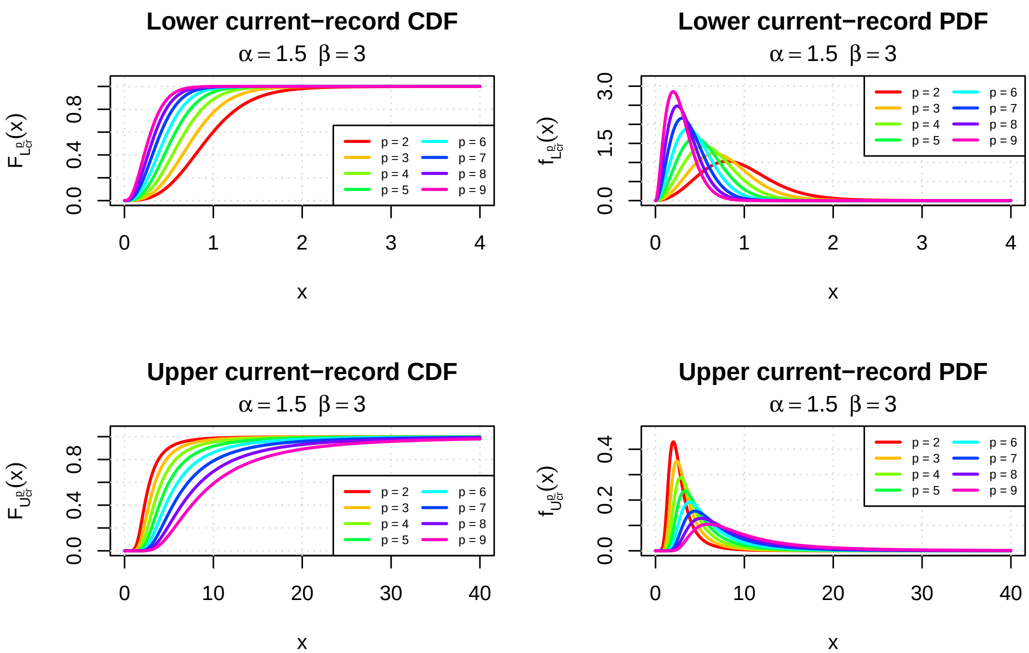

Figure 2. PDF and CDF of upper and lower current records for $\hat{\alpha} = 1.5$ and $\hat{\beta} = 3$.

A similar pattern is observed for the upper current records. As the record number p increases, the upper current-record CDFs shift to the right, implying that larger values are required before higher-order upper records are observed. Likewise, the corresponding PDFs remain positively skewed, with their modes moving toward larger values of x, illustrating the increasing magnitude of successive upper current records.

Comparing Figures 1–3 also demonstrates the influence of the Log-Logistic parameters. Increasing the scale parameter α shifts both the upper and lower current-record distributions toward larger values of x, while increasing the shape parameter β produces steeper cumulative distribution functions and more concentrated probability density functions. Consequently, larger values of β reduce the dispersion of both upper and lower current records while preserving their general probabilistic characteristics. Overall, the figures demonstrate the flexibility of the proposed current-record distributions and confirm that they exhibit the expected behavior under different parameter settings. The derived distribution functions also permit direct evaluation of probabilities associated with upper and lower current-record levels. For example, for a specified pressure threshold x, the probabilities $P(U_{cr}^p \leq x)$ and $P(L_{cr}^p \leq x)$ are obtained directly from the corresponding CDFs. Hence, exceedance or non-exceedance probabilities for current-record pressure levels can be evaluated without requiring an additional probability model.

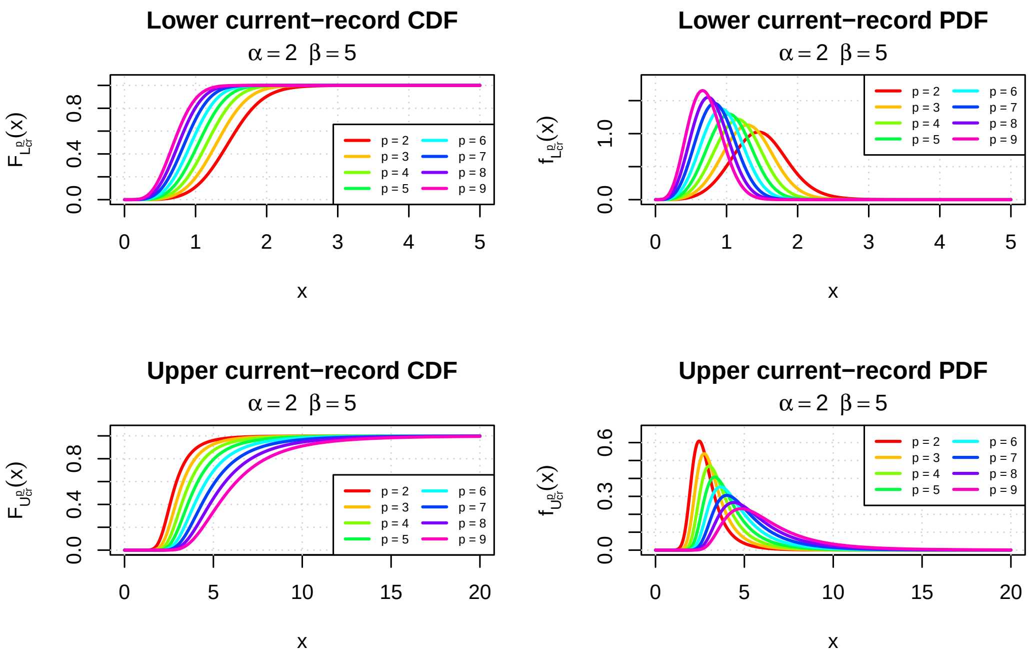

Figure 3. PDF and CDF of upper and lower current records for $\hat{\alpha} = 2$ and $\hat{\beta} = 5$.

3. Joint and conditional density functions

The joint density of the lower current records is obtained by substituting the Log-Logistic PDF (2) and CDF (1) into the general current-record formula given by [13]

$$f_{L_{\tilde{cr}}^p, L_{\tilde{cr}}^q}(l_p, l_q) = \frac{f(l_p) f(l_q)}{F(l_p)(q-p-1)!} \Big(H(l_p) - H(l_q) \Big)^{q-p-1}.$$

Thus,

$$f_{L^p_{\tilde{cr}},L^q_{\tilde{cr}}}(l_p,l_q)=\frac{\beta^2\alpha^{2\beta}l_q^{\beta-1}}{l_p(\alpha^\beta+l_p^\beta)(\alpha^\beta+l_q^\beta)^2(q-p-1)!}\left[\log\left(\frac{l_p^\beta(\alpha^\beta+l_q^\beta)}{l_q^\beta(\alpha^\beta+l_p^\beta)}\right)\right]^{q-p-1},\qquad l_q<l_p. \tag{8}$$

Similarly, the conditional density of the lower current records is obtained from

$$f_{L^q_{\tilde{cr}}|L^p_{\tilde{cr}}}(l_q|l_p)=\frac{f(l_q)}{F(l_p)(q-p-1)!}\Big(H(l_p)-H(l_q)\Big)^{q-p-1}.$$

which becomes

$$f_{L^q_{\tilde{cr}}|L^p_{\tilde{cr}}}(l_q|l_p)=\frac{\beta\alpha^\beta(\alpha^\beta+l_p^\beta)l_q^{\beta-1}}{l_p^\beta(\alpha^\beta+l_q^\beta)^2(q-p-1)!}\left[\log\left(\frac{l_p^\beta(\alpha^\beta+l_q^\beta)}{l_q^\beta(\alpha^\beta+l_p^\beta)}\right)\right]^{q-p-1},\qquad l_q<l_p. \tag{9}$$

For the upper current records, we use

$$f_{U^p_{\tilde{cr}},U^q_{\tilde{cr}}}(u_p,u_q)=\frac{f(u_p)f(u_q)}{\bar{F}(u_p)(q-p-1)!}\Big(R(u_q)-R(u_p)\Big)^{q-p-1}.$$

Substituting the Log-Logistic PDF and survival function yields

$$f_{U^p_{\tilde{cr}},U^q_{\tilde{cr}}}(u_p,u_q)=\frac{\beta^2\alpha^\beta u_p^{\beta-1}u_q^{\beta-1}}{(\alpha^\beta+u_p^\beta)(\alpha^\beta+u_q^\beta)^2(q-p-1)!}\left[\log\left(\frac{\alpha^\beta+u_q^\beta}{\alpha^\beta+u_p^\beta}\right)\right]^{q-p-1},\qquad u_q>u_p. \tag{10}$$

Likewise, the conditional density is

$$f_{U^q_{\tilde{cr}}|U^p_{\tilde{cr}}}(u_q|u_p)=\frac{f(u_q)}{\bar{F}(u_p)(q-p-1)!}\Big(R(u_q)-R(u_p)\Big)^{q-p-1}.$$

which becomes

$$f_{U^q_{\tilde{cr}}|U^p_{\tilde{cr}}}(u_q|u_p)=\frac{\beta(\alpha^\beta+u_p^\beta)u_q^{\beta-1}}{(\alpha^\beta+u_q^\beta)^2(q-p-1)!}\left[\log\left(\frac{\alpha^\beta+u_q^\beta}{\alpha^\beta+u_p^\beta}\right)\right]^{q-p-1},\qquad u_q>u_p. \tag{11}$$

4. Moments, Entropy and Extropy

The moments, entropy, and extropy of the proposed Log-Logistic current-record distributions provide useful measures for describing their location, variability, uncertainty, and information content. Since the probability density functions of the upper and lower current records have been obtained explicitly in Section 2, these quantities can be derived directly from their corresponding density functions.

In the context of atmospheric-pressure current records, Shannon entropy provides a measure of the uncertainty associated with the possible values of future or sequential record pressures. A relatively high entropy corresponds to a more dispersed current-record distribution and therefore greater uncertainty in the pressure level at which a subsequent record may occur, whereas lower entropy indicates a more concentrated and predictable record distribution. Extropy provides a complementary measure of this uncertainty by emphasizing the concentration of the probability density and can therefore help characterize differences in the dispersion of record-pressure distributions. These measures should be interpreted statistically rather than as direct indicators of particular weather conditions. In particular, a higher entropy does not by itself imply severe weather or long-term climate change in Riyadh; it indicates greater uncertainty or variability in the modeled atmospheric-pressure current-record process.

The r^{th} raw moment of the lower current record is obtained from

$$\delta^r_{L^p_{\tilde{c}r}} = E(L^r_{\tilde{c}r}) = 2^p \int_0^\infty x^r f(x) G(p, -\log F(x))\, dx.$$

Substituting the Log-Logistic density and distribution functions yields

$$\delta^r_{L^p_{\tilde{c}r}} = 2^p \beta\alpha^\beta \int_0^\infty \frac{x^{r+\beta-1}}{(\alpha^\beta + x^\beta)^2} G\left(p, \log\left(1 + \left(\frac{\alpha}{x}\right)^\beta\right)\right) dx. \tag{12}$$

Similarly, the r^{th} raw moment of the upper current record is

$$\delta^r_{U^p_{\tilde{c}r}} = 2^p \beta\alpha^\beta \int_0^\infty \frac{x^{r+\beta-1}}{(\alpha^\beta + x^\beta)^2} G\left(p, \log\left(1 + \left(\frac{x}{\alpha}\right)^\beta\right)\right) dx. \tag{13}$$

The Shannon entropy [20] of the lower current records is

$$H(L^p_{\tilde{c}r}) = -\int_0^\infty f_{L^p_{\tilde{c}r}}(x) \log f_{L^p_{\tilde{c}r}}(x) dx,$$

which becomes

$$\begin{aligned} H(L^p_{\tilde{c}r}) = -p\log 2 - 2^p \beta\alpha^\beta \int_0^\infty & \frac{x^{\beta-1}}{(\alpha^\beta + x^\beta)^2} G\left(p, \log\left(1 + \left(\frac{\alpha}{x}\right)^\beta\right)\right) \\ & \times \log\left[\frac{\beta\alpha^\beta x^{\beta-1}}{(\alpha^\beta + x^\beta)^2} G\left(p, \log\left(1 + \left(\frac{\alpha}{x}\right)^\beta\right)\right)\right] dx. \end{aligned} \tag{14}$$

Likewise, the entropy of the upper current records is

$$\begin{aligned} H(U^p_{\tilde{c}r}) = -p\log 2 - 2^p \beta\alpha^\beta \int_0^\infty & \frac{x^{\beta-1}}{(\alpha^\beta + x^\beta)^2} G\left(p, \log\left(1 + \left(\frac{x}{\alpha}\right)^\beta\right)\right) \\ & \times \log\left[\frac{\beta\alpha^\beta x^{\beta-1}}{(\alpha^\beta + x^\beta)^2} G\left(p, \log\left(1 + \left(\frac{x}{\alpha}\right)^\beta\right)\right)\right] dx. \end{aligned} \tag{15}$$

Finally, the extropy of the lower and upper current records established by [14] is given, respectively, by

$$\begin{aligned} J(L^p_{\tilde{c}r}) &= -\frac{1}{2}\int_0^\infty f^2_{L^p_{\tilde{c}r}}(x) dx \\ &= -2^{2p-1}\beta^2\alpha^{2\beta} \int_0^\infty \frac{x^{2\beta-2}}{(\alpha^\beta + x^\beta)^4} G^2\left(p, \log\left(1 + \left(\frac{\alpha}{x}\right)^\beta\right)\right) dx, \end{aligned} \tag{16}$$

$$J(U^p_{\tilde{c}r}) = -2^{2p-1}\beta^2\alpha^{2\beta} \int_0^\infty \frac{x^{2\beta-2}}{(\alpha^\beta + x^\beta)^4} G^2\left(p, \log\left(1 + \left(\frac{x}{\alpha}\right)^\beta\right)\right) dx. \tag{17}$$

5. Estimation using the new PDFs

In this section, the unknown parameters α and β of the Log-Logistic distribution are estimated directly from the newly derived current-record density functions. Unlike classical inference based on complete random samples, the proposed approach utilizes only the observed upper or lower current records. Consequently, the likelihood functions are constructed from the gamma-based current-record probability density functions derived in Section 2.

5.1. Maximum likelihood estimation

Suppose that $U^1_{\tilde{c}r}, U^2_{\tilde{c}r}, \dots, U^p_{\tilde{c}r}$ denote the observed upper current records. Using Equation (7), the likelihood function is

$$L_{U^p_{\tilde{c}r}}(\alpha,\beta) = \prod_{i=1}^{p} \frac{2^i \beta \alpha^\beta u_i^{\beta-1}}{(\alpha^\beta + u_i^\beta)^2} G\left(i, \log\left(1 + \left(\frac{u_i}{\alpha}\right)^\beta\right)\right). \tag{18}$$

Therefore, the corresponding log-likelihood function is

$$\ell_{U^p_{\tilde{c}r}}(\alpha,\beta) = \sum_{i=1}^{p} \Bigg[i\log 2 + \log\beta + \beta\log\alpha + (\beta-1)\log u_i - 2\log(\alpha^\beta + u_i^\beta) + \log G(T_i) \Bigg], \tag{19}$$

where $T_i = \log\left(1 + \left(\frac{u_i}{\alpha}\right)^\beta\right)$. Similarly, let $L^1_{\tilde{c}r}, L^2_{\tilde{c}r}, \dots, L^p_{\tilde{c}r}$ be the observed lower-current records. Using Equation (5), the likelihood function is

$$L_{L^p_{\tilde{c}r}}(\alpha,\beta) = \prod_{i=1}^{p} \frac{2^i \beta \alpha^\beta l_i^{\beta-1}}{(\alpha^\beta + l_i^\beta)^2} G\left(i, \log\left(1 + \left(\frac{\alpha}{l_i}\right)^\beta\right)\right). \tag{20}$$

Hence,

$$\ell_{L^p_{\tilde{c}r}}(\alpha,\beta) = \sum_{i=1}^{p} \Bigg[i\log 2 + \log\beta + \beta\log\alpha + (\beta-1)\log l_i - 2\log(\alpha^\beta + l_i^\beta) + \log G(S_i) \Bigg], \tag{21}$$

where $S_i = \log\left(1 + \left(\frac{\alpha}{l_i}\right)^\beta\right)$.

The maximum likelihood estimates of α and β are obtained by maximizing the corresponding log-likelihood functions. Differentiating the upper log-likelihood with respect to the unknown parameters yields

$$\frac{\partial \ell_{U^p_{\tilde{c}r}}}{\partial \alpha} = 0, \qquad \frac{\partial \ell_{U^p_{\tilde{c}r}}}{\partial \beta} = 0,$$

while the likelihood equations for the lower current records are

$$\frac{\partial \ell_{L^p_{\tilde{c}r}}}{\partial \alpha} = 0, \qquad \frac{\partial \ell_{L^p_{\tilde{c}r}}}{\partial \beta} = 0.$$

Since these equations contain nonlinear terms involving the regularized incomplete gamma function, explicit solutions do not exist. Therefore, the maximum likelihood estimates are obtained numerically using iterative optimization algorithms such as the Newton–Raphson method or quasi-Newton optimization.

5.2. BE under new PDF

For Bayesian estimation, we assume that α and β are independent gamma random variables with prior densities

$$\pi(\alpha) \propto \alpha^{a_1-1}\exp(-b_1\alpha), \qquad \alpha > 0, \qquad \pi(\beta) \propto \beta^{a_2-1}\exp(-b_2\beta), \qquad \beta > 0.$$

Thus, the joint prior density is

$$\pi(\alpha,\beta) \propto \alpha^{a_1-1}\beta^{a_2-1}\exp(-b_1\alpha - b_2\beta).$$

Using the upper current-record likelihood (18), the posterior density is

$$\pi_{U^p_{\tilde{c}r}}(\alpha,\beta \mid \mathbf{u}) \propto L_{U^p_{\tilde{c}r}}(\alpha,\beta)\pi(\alpha,\beta). \tag{22}$$

Similarly, using the lower current-record likelihood (20), the posterior density is

$$\pi_{L^p_{\tilde{c}r}}(\alpha,\beta \mid \mathbf{l}) \propto L_{L^p_{\tilde{c}r}}(\alpha,\beta)\pi(\alpha,\beta). \tag{23}$$

Under the squared error loss function, the Bayes estimators are the posterior means:

$$\hat{\alpha}^{BE}_{U_{\tilde{c}r}} = E(\alpha \mid \mathbf{u}), \hat{\beta}^{BE}_{U_{\tilde{c}r}} = E(\beta \mid \mathbf{u}), \qquad \hat{\alpha}^{BE}_{L_{\tilde{c}r}} = E(\alpha \mid \mathbf{l}), \hat{\beta}^{BE}_{L_{\tilde{c}r}} = E(\beta \mid \mathbf{l}). \tag{24}$$

Since these posterior expectations cannot be obtained in closed form, Markov Chain Monte Carlo methods may be used to approximate them. If $(\alpha^{(t)},\beta^{(t)})$, $t=1,\ldots,T$, are posterior samples after burn-in, then

$$\hat{\alpha}^{BE} = \frac{1}{T}\sum_{t=1}^{T}\alpha^{(t)}, \qquad \hat{\beta}^{BE} = \frac{1}{T}\sum_{t=1}^{T}\beta^{(t)}.$$

The corresponding credible intervals are obtained from the empirical posterior quantiles.

6. Simulation

To evaluate the finite-sample performance of the proposed estimation procedures, a Monte Carlo simulation study was conducted. Following the structure of the simulation study in the related current-record paper, 1000 random samples of size 100 were generated from the Log-Logistic distribution for selected values of the parameters α and β. For each generated sample, the corresponding upper and lower current records were extracted. The unknown parameters were then estimated using maximum-likelihood and Bayesian methods based on the newly derived current-record density functions.

The likelihood functions used in the simulation were derived from the proposed gamma-based PDFs for the upper and lower current records. Since the likelihood equations involve the regularized incomplete gamma function and do not admit closed-form solutions, the maximum likelihood estimates were obtained numerically using constrained optimization techniques. For Bayesian estimation, independent Gamma prior distributions were assumed for the unknown parameters, and posterior samples were generated using the Metropolis–Hastings algorithm. Under the squared-error loss function, the Bayesian estimates were computed as the posterior means.

To assess the performance of the proposed estimators, the mean estimate, standard deviation (SD), root mean square error (RMSE), and mean absolute deviation (MAD) were calculated over the 1000 simulation replications. In addition, 95% confidence intervals for the maximum likelihood estimators and 95% credible intervals for the Bayesian estimators were constructed using the empirical quantiles of the simulated estimates. The simulation results are presented in Tables 1–3, in which the performance of the maximum-likelihood and Bayesian methods is compared for both upper and lower current records under different parameter settings. In Tables 1–3, e denotes the number of Monte Carlo replications, out of the 1000 generated samples, that resulted in the corresponding current-record number p.

Table 1. Simulation results for the Log-Logistic current-record model when $\alpha = 1$ and $\beta = 2$.

		MLE					BE				
p	Parameter	Mean	SD	RMSE	MAD	95% CI	Mean	SD	RMSE	MAD	95% BCI
4 ($e = 10$)	$\alpha_{U_{\tilde{c}r}}$	3.1251	3.8851	4.2347	2.5032	[0.2467, 0.5668]	1.3688	0.5850	0.6635	0.5647	[0.6351, 0.7853]
	$\beta_{U_{\tilde{c}r}}$	1.8836	0.8680	0.8266	0.7831	[0.6515, 1.1265]	1.3759	0.4666	0.7636	0.6241	[0.7575, 1.0331]
	$\alpha_{L_{\tilde{c}r}}$	2.0062	2.4318	2.5038	1.4983	[0.2780, 0.4937]	1.0893	0.5413	0.5181	0.4518	[0.4686, 0.6577]
	$\beta_{L_{\tilde{c}r}}$	1.5281	0.8040	0.8930	0.8555	[0.7236, 0.9073]	1.3806	0.4266	0.7385	0.6324	[0.8921, 1.0681]
5 ($e = 40$)	$\alpha_{U_{\tilde{c}r}}$	1.7359	2.0940	2.1947	1.1524	[0.1952, 0.6211]	1.1709	0.6242	0.6396	0.4726	[0.3008, 0.7055]
	$\beta_{U_{\tilde{c}r}}$	1.7250	0.6962	0.7404	0.6579	[0.7235, 1.0757]	1.4897	0.4006	0.6456	0.5332	[0.8051, 1.1515]
	$\alpha_{L_{\tilde{c}r}}$	1.2659	1.5010	1.5058	0.8574	[0.0683, 0.3933]	1.0302	0.5053	0.4998	0.4183	[0.2163, 0.6253]
	$\beta_{L_{\tilde{c}r}}$	1.9505	0.6878	0.6809	0.6173	[0.8354, 1.2759]	1.6740	0.3776	0.4953	0.3519	[0.9180, 1.3826]
6 ($e = 64$)	$\alpha_{U_{\tilde{c}r}}$	1.4611	1.1964	1.2734	0.8395	[0.1073, 0.6316]	1.1274	0.5454	0.5559	0.4452	[0.2295, 0.7329]
	$\beta_{U_{\tilde{c}r}}$	1.8698	0.5665	0.5770	0.5119	[0.7614, 1.4307]	1.6478	0.3263	0.4785	0.3759	[0.9017, 1.4022]
	$\alpha_{L_{\tilde{c}r}}$	1.0938	0.8240	0.8229	0.6441	[0.1364, 0.4618]	1.1005	0.5093	0.5152	0.4341	[0.2930, 0.7325]
	$\beta_{L_{\tilde{c}r}}$	1.9763	0.5541	0.5502	0.4919	[0.8265, 1.5200]	1.7514	0.3311	0.4119	0.3174	[0.8509, 1.5230]
7 ($e = 132$)	$\alpha_{U_{\tilde{c}r}}$	1.4180	1.1161	1.1879	0.7292	[0.2201, 0.6957]	1.1133	0.5339	0.5438	0.4137	[0.2723, 0.7418]
	$\beta_{U_{\tilde{c}r}}$	2.0403	0.5272	0.5268	0.4778	[0.8180, 1.5803]	1.7953	0.3244	0.3826	0.2950	[0.8112, 1.5527]
	$\alpha_{L_{\tilde{c}r}}$	1.2530	1.0551	1.0811	0.7115	[0.2246, 0.5622]	1.1887	0.5651	0.5937	0.4436	[0.3985, 0.7710]
	$\beta_{L_{\tilde{c}r}}$	2.0835	0.5232	0.5278	0.4833	[0.9981, 1.5677]	1.8819	0.2961	0.3178	0.2477	[1.1085, 1.6301]
8 ($e = 123$)	$\alpha_{U_{\tilde{c}r}}$	1.1175	0.8687	0.8731	0.5106	[0.0931, 0.6097]	0.9407	0.4638	0.4657	0.3474	[0.1893, 0.6410]
	$\beta_{U_{\tilde{c}r}}$	2.1416	0.4937	0.5116	0.4505	[0.9355, 1.7982]	1.9280	0.3224	0.3291	0.2480	[0.8923, 1.7971]
	$\alpha_{L_{\tilde{c}r}}$	1.1133	0.8186	0.8231	0.5031	[0.1065, 0.5966]	1.1613	0.4978	0.5214	0.3914	[0.1550, 0.7773]
	$\beta_{L_{\tilde{c}r}}$	2.2054	0.4570	0.4993	0.4441	[1.1179, 1.9114]	1.9879	0.2810	0.2801	0.2235	[1.1772, 1.8385]
9 ($e = 169$)	$\alpha_{U_{\tilde{c}r}}$	1.0661	0.6535	0.6549	0.4340	[0.1387, 0.6713]	0.9195	0.4055	0.4123	0.3282	[0.1812, 0.6520]
	$\beta_{U_{\tilde{c}r}}$	2.2210	0.4041	0.4595	0.4053	[1.1969, 1.8937]	2.0079	0.2685	0.2679	0.2232	[1.2263, 1.8293]
	$\alpha_{L_{\tilde{c}r}}$	1.1306	0.6498	0.6609	0.4290	[0.2000, 0.7372]	1.2426	0.4956	0.5505	0.4018	[0.3162, 0.9125]
	$\beta_{L_{\tilde{c}r}}$	2.3703	0.3141	0.4850	0.4336	[1.3886, 2.1174]	2.1430	0.1940	0.2406	0.2070	[1.4052, 2.0296]
10 ($e = 151$)	$\alpha_{U_{\tilde{c}r}}$	1.0599	0.6279	0.6286	0.4130	[0.1526, 0.6543]	0.9162	0.4115	0.4187	0.3210	[0.1718, 0.6244]
	$\beta_{U_{\tilde{c}r}}$	2.3441	0.3552	0.4937	0.4504	[1.2305, 2.1230]	2.1283	0.2435	0.2745	0.2403	[1.1426, 2.0064]
	$\alpha_{L_{\tilde{c}r}}$	1.2840	0.7819	0.8294	0.5249	[0.3202, 0.8272]	1.3487	0.5790	0.6743	0.4885	[0.4161, 0.9750]
	$\beta_{L_{\tilde{c}r}}$	2.3697	0.3447	0.5047	0.4639	[1.2896, 2.1651]	2.1781	0.2204	0.2828	0.2537	[1.3597, 2.0666]
11 ($e = 120$)	$\alpha_{U_{\tilde{c}r}}$	0.8843	0.3972	0.4121	0.3044	[0.2167, 0.6701]	0.7838	0.2946	0.3645	0.2985	[0.2528, 0.6164]
	$\beta_{U_{\tilde{c}r}}$	2.4460	0.2986	0.5360	0.5104	[1.3269, 2.4643]	2.2212	0.2104	0.3047	0.2827	[1.3460, 2.1699]
	$\alpha_{L_{\tilde{c}r}}$	1.2828	0.8157	0.8601	0.4454	[0.3378, 0.8940]	1.3797	0.5528	0.6687	0.4637	[0.4579, 1.0718]
	$\beta_{L_{\tilde{c}r}}$	2.4903	0.2500	0.5499	0.5265	[1.5406, 2.6000]	2.2817	0.1619	0.3246	0.3071	[1.5829, 2.2559]
12 ($e = 73$)	$\alpha_{U_{\tilde{c}r}}$	0.7979	0.2844	0.3473	0.3001	[0.3371, 0.5993]	0.7277	0.2395	0.3616	0.3253	[0.3503, 0.5596]
	$\beta_{U_{\tilde{c}r}}$	2.4866	0.2118	0.5301	0.5011	[1.7518, 2.4377]	2.2958	0.1561	0.3340	0.3145	[1.6971, 2.2141]
	$\alpha_{L_{\tilde{c}r}}$	1.3544	0.5514	0.6523	0.4546	[0.4074, 1.0174]	1.4749	0.4779	0.6714	0.5367	[0.5061, 1.2006]
	$\beta_{L_{\tilde{c}r}}$	2.4766	0.2495	0.5371	0.5116	[1.4830, 2.4747]	2.2940	0.1748	0.3414	0.3223	[1.5284, 2.2477]
13 ($e = 57$)	$\alpha_{U_{\tilde{c}r}}$	0.7644	0.2091	0.3138	0.2714	[0.3872, 0.6506]	0.7051	0.1803	0.3448	0.3152	[0.3703, 0.6076]
	$\beta_{U_{\tilde{c}r}}$	2.5160	0.2120	0.5572	0.5402	[1.5018, 2.6000]	2.3435	0.1638	0.3799	0.3658	[1.5352, 2.3487]
	$\alpha_{L_{\tilde{c}r}}$	1.4755	0.4533	0.6542	0.5089	[0.5707, 1.1321]	1.6040	0.4281	0.7382	0.6232	[0.7223, 1.3035]
	$\beta_{L_{\tilde{c}r}}$	2.5360	0.1577	0.5583	0.5457	[1.7241, 2.6000]	2.3663	0.1254	0.3869	0.3764	[1.7147, 2.3200]
14 ($e = 32$)	$\alpha_{U_{\tilde{c}r}}$	0.6221	0.1733	0.4146	0.3869	[0.2939, 0.5056]	0.5732	0.1581	0.4543	0.4290	[0.2626, 0.4717]
	$\beta_{U_{\tilde{c}r}}$	2.5795	0.1025	0.5883	0.5795	[2.0227, 2.6000]	2.4025	0.0852	0.4112	0.4025	[2.0207, 2.3927]
	$\alpha_{L_{\tilde{c}r}}$	1.5007	0.4705	0.6820	0.5570	[0.6786, 1.2012]	1.6117	0.4338	0.7459	0.6326	[0.8336, 1.3129]
	$\beta_{L_{\tilde{c}r}}$	2.5594	0.1757	0.5855	0.5827	[1.6271, 2.6000]	2.4123	0.1266	0.4307	0.4251	[1.7946, 2.4156]
15 ($e = 14$)	$\alpha_{U_{\tilde{c}r}}$	0.6884	0.2494	0.3935	0.3688	[0.3705, 0.5326]	0.6348	0.2271	0.4257	0.3922	[0.3329, 0.4937]
	$\beta_{U_{\tilde{c}r}}$	2.6000	0.0000	0.6000	0.6000	[2.6000, 2.6000]	2.4422	0.0304	0.4432	0.4422	[2.3654, 2.4233]
	$\alpha_{L_{\tilde{c}r}}$	1.9490	0.6980	1.1632	0.9700	[0.8534, 1.3944]	2.0678	0.6315	1.2290	1.0678	[1.0621, 1.5700]
	$\beta_{L_{\tilde{c}r}}$	2.5995	0.0020	0.5995	0.5995	[2.5927, 2.6000]	2.4391	0.0446	0.4412	0.4391	[2.3116, 2.4241]
16 ($e = 7$)	$\alpha_{U_{\tilde{c}r}}$	0.6589	0.2026	0.3893	0.3411	[0.4383, 0.4802]	0.6250	0.1910	0.4146	0.3750	[0.4071, 0.4644]
	$\beta_{U_{\tilde{c}r}}$	2.5425	0.1522	0.5605	0.5425	[2.1972, 2.6000]	2.4182	0.1290	0.4349	0.4182	[2.1341, 2.4284]
	$\alpha_{L_{\tilde{c}r}}$	1.6549	0.3987	0.7517	0.6593	[0.9846, 1.5220]	1.7384	0.3630	0.8112	0.7384	[1.0827, 1.6476]
	$\beta_{L_{\tilde{c}r}}$	2.4875	0.2977	0.5600	0.5411	[1.8124, 2.6000]	2.3916	0.2669	0.4631	0.4525	[1.7867, 2.4807]
17 ($e = 8$)	$\alpha_{U_{\tilde{c}r}}$	0.5724	0.2027	0.4659	0.4276	[0.3601, 0.4417]	0.5522	0.1876	0.4795	0.4478	[0.3479, 0.4456]
	$\beta_{U_{\tilde{c}r}}$	2.5485	0.1261	0.5605	0.5485	[2.2910, 2.6000]	2.4489	0.1009	0.4582	0.4489	[2.2462, 2.4654]
	$\alpha_{L_{\tilde{c}r}}$	2.0356	0.4226	1.1051	1.0356	[1.4703, 1.6846]	2.0904	0.4078	1.1522	1.0904	[1.5124, 1.7818]
	$\beta_{L_{\tilde{c}r}}$	2.6000	0.0000	0.6000	0.6000	[2.6000, 2.6000]	2.5007	0.0112	0.5008	0.5007	[2.4840, 2.4940]

Table 2. Simulation results for the Log-Logistic current-record model when $\alpha = 1.5$ and $\beta = 3$.

		MLE					BE				
p	Parameter	Mean	SD	RMSE	MAD	95% CI	Mean	SD	RMSE	MAD	95% BCI
4 ($e = 8$)	$\alpha_{U_{\tilde{c}r}}$	1.7442	1.2542	1.1707	0.9824	[0.4350, 0.9143]	1.5850	0.8486	0.7793	0.6592	[0.7146, 1.0201]
	$\beta_{U_{\tilde{c}r}}$	2.5598	1.1942	1.1757	1.0402	[1.2467, 1.5972]	2.2049	0.6458	0.9898	0.7951	[1.4478, 1.6664]
	$\alpha_{L_{\tilde{c}r}}$	1.2677	0.6705	0.6547	0.5507	[0.3322, 0.8688]	1.4018	0.4675	0.4379	0.3784	[0.6434, 1.1946]
	$\beta_{L_{\tilde{c}r}}$	2.7800	1.1274	1.0524	0.9356	[1.3879, 1.8019]	2.2327	0.5328	0.9085	0.7673	[1.5173, 1.8341]
5 ($e = 30$)	$\alpha_{U_{\tilde{c}r}}$	2.2689	1.7978	1.9276	1.1487	[0.6578, 1.2035]	1.8598	1.0126	1.0586	0.7481	[0.6998, 1.0885]
	$\beta_{U_{\tilde{c}r}}$	2.9196	0.9856	0.9724	0.8409	[0.8779, 2.1614]	2.4494	0.6014	0.8079	0.5853	[0.9235, 2.1592]
	$\alpha_{L_{\tilde{c}r}}$	1.9565	1.2635	1.3234	0.9086	[0.5415, 1.1216]	1.8439	0.6563	0.7311	0.5898	[0.7559, 1.3775]
	$\beta_{L_{\tilde{c}r}}$	2.5235	0.9755	1.0710	0.9527	[1.1675, 1.7350]	2.2768	0.5637	0.9112	0.7391	[1.3219, 1.8855]
6 ($e = 74$)	$\alpha_{U_{\tilde{c}r}}$	1.6466	0.8678	0.8743	0.6711	[0.3172, 0.9280]	1.4999	0.6419	0.6375	0.5027	[0.3903, 1.0030]
	$\beta_{U_{\tilde{c}r}}$	2.7536	0.8536	0.8829	0.8075	[1.4071, 2.0376]	2.4801	0.5253	0.7366	0.6115	[1.5522, 2.0334]
	$\alpha_{L_{\tilde{c}r}}$	1.4089	0.8970	0.8955	0.6400	[0.3228, 0.8770]	1.5072	0.6463	0.6420	0.4836	[0.4143, 1.1020]
	$\beta_{L_{\tilde{c}r}}$	3.0807	0.8680	0.8658	0.7874	[1.4156, 2.1841]	2.6839	0.5159	0.6021	0.4492	[1.5963, 2.2046]
7 ($e = 93$)	$\alpha_{U_{\tilde{c}r}}$	1.7196	0.8929	0.9148	0.6664	[0.5276, 1.0303]	1.5293	0.6551	0.6523	0.5088	[0.6108, 1.0449]
	$\beta_{U_{\tilde{c}r}}$	3.0953	0.8030	0.8043	0.7403	[1.5546, 2.3763]	2.7226	0.4982	0.5679	0.4456	[1.7084, 2.3074]
	$\alpha_{L_{\tilde{c}r}}$	1.5913	0.8364	0.8369	0.6362	[0.4052, 0.9716]	1.6690	0.6477	0.6660	0.5280	[0.4960, 1.1594]
	$\beta_{L_{\tilde{c}r}}$	3.0608	0.8094	0.8073	0.7062	[1.3024, 2.3525]	2.7557	0.5175	0.5697	0.4222	[1.3600, 2.4058]
8 ($e = 166$)	$\alpha_{U_{\tilde{c}r}}$	1.6330	0.7657	0.7749	0.5085	[0.5692, 1.1747]	1.4761	0.5816	0.5803	0.4060	[0.6021, 1.0977]
	$\beta_{U_{\tilde{c}r}}$	3.2807	0.6872	0.7404	0.6768	[1.7267, 2.6727]	2.9297	0.4609	0.4649	0.3902	[1.7809, 2.5756]
	$\alpha_{L_{\tilde{c}r}}$	1.5928	0.6540	0.6586	0.4681	[0.5093, 1.1711]	1.7198	0.5237	0.5665	0.4335	[0.6512, 1.3340]
	$\beta_{L_{\tilde{c}r}}$	3.2593	0.6857	0.7311	0.6561	[1.5196, 2.7307]	2.9368	0.4237	0.4271	0.3414	[1.7371, 2.6486]
9 ($e = 154$)	$\alpha_{U_{\tilde{c}r}}$	1.5141	0.5193	0.5178	0.4018	[0.5356, 1.1737]	1.3843	0.4215	0.4357	0.3575	[0.6219, 1.0893]
	$\beta_{U_{\tilde{c}r}}$	3.4197	0.6352	0.7596	0.6919	[1.5290, 2.9687]	3.0675	0.4383	0.4421	0.3666	[1.4424, 2.8682]
	$\alpha_{L_{\tilde{c}r}}$	1.6034	0.5576	0.5653	0.4192	[0.4877, 1.2366]	1.7551	0.4999	0.5598	0.4166	[0.5806, 1.4420]
	$\beta_{L_{\tilde{c}r}}$	3.4287	0.5643	0.7072	0.6318	[2.0117, 3.0115]	3.1022	0.3643	0.3772	0.3245	[2.1199, 2.8940]
10 ($e = 158$)	$\alpha_{U_{\tilde{c}r}}$	1.4960	0.4306	0.4292	0.3143	[0.4193, 1.2209]	1.3630	0.3589	0.3831	0.3082	[0.4978, 1.1215]
	$\beta_{U_{\tilde{c}r}}$	3.6522	0.4042	0.7667	0.7124	[2.1091, 3.4499]	3.2829	0.2832	0.3996	0.3555	[2.2926, 3.1242]
	$\alpha_{L_{\tilde{c}r}}$	1.7387	0.4906	0.5442	0.4005	[0.3603, 1.4046]	1.9098	0.4723	0.6241	0.4835	[0.4448, 1.5832]
	$\beta_{L_{\tilde{c}r}}$	3.5366	0.4847	0.7220	0.6506	[2.0722, 3.1457]	3.2147	0.3295	0.3924	0.3412	[2.0589, 3.0418]
11 ($e = 118$)	$\alpha_{U_{\tilde{c}r}}$	1.3307	0.3603	0.3967	0.3154	[0.4329, 1.1276]	1.2224	0.3044	0.4110	0.3522	[0.5161, 1.0414]
	$\beta_{U_{\tilde{c}r}}$	3.6652	0.4134	0.7822	0.7315	[2.2628, 3.6230]	3.3268	0.2866	0.4339	0.3987	[2.3738, 3.1994]
	$\alpha_{L_{\tilde{c}r}}$	1.6862	0.4785	0.5115	0.3857	[0.3895, 1.3276]	1.8473	0.4695	0.5824	0.4540	[0.4476, 1.4749]
	$\beta_{L_{\tilde{c}r}}$	3.6999	0.3819	0.7965	0.7635	[2.1422, 3.6143]	3.3720	0.2755	0.4623	0.4332	[2.2272, 3.2829]
12 ($e = 90$)	$\alpha_{U_{\tilde{c}r}}$	1.3523	0.4273	0.4499	0.3202	[0.5416, 1.1472]	1.2462	0.3554	0.4351	0.3481	[0.5390, 1.0524]
	$\beta_{U_{\tilde{c}r}}$	3.8088	0.2410	0.8436	0.8186	[2.7458, 3.9000]	3.4866	0.1901	0.5220	0.5002	[2.6836, 3.4234]
	$\alpha_{L_{\tilde{c}r}}$	1.8080	0.4960	0.5815	0.4128	[0.8058, 1.4933]	1.9573	0.4743	0.6569	0.5142	[0.9097, 1.6461]
	$\beta_{L_{\tilde{c}r}}$	3.6901	0.4003	0.7967	0.7494	[2.2452, 3.6943]	3.4090	0.2968	0.5043	0.4685	[2.2740, 3.3212]
13 ($e = 56$)	$\alpha_{U_{\tilde{c}r}}$	1.2210	0.2291	0.3597	0.3077	[0.7657, 1.0769]	1.1304	0.2027	0.4207	0.3748	[0.7258, 1.0071]
	$\beta_{U_{\tilde{c}r}}$	3.8342	0.2164	0.8613	0.8499	[2.5590, 3.9000]	3.5290	0.1846	0.5598	0.5446	[2.5654, 3.4722]
	$\alpha_{L_{\tilde{c}r}}$	1.9254	0.3684	0.5606	0.4561	[1.2814, 1.6497]	2.0795	0.3755	0.6887	0.5854	[1.3919, 1.7903]
	$\beta_{L_{\tilde{c}r}}$	3.7970	0.2689	0.8404	0.8063	[2.8138, 3.9000]	3.5367	0.2129	0.5767	0.5519	[2.7884, 3.5486]
14 ($e = 26$)	$\alpha_{U_{\tilde{c}r}}$	1.2233	0.2799	0.3898	0.3410	[0.7800, 1.0258]	1.1371	0.2556	0.4410	0.3898	[0.7333, 0.9504]
	$\beta_{U_{\tilde{c}r}}$	3.8705	0.0849	0.8745	0.8705	[3.5826, 3.9000]	3.5998	0.1108	0.6095	0.5998	[3.2659, 3.5932]
	$\alpha_{L_{\tilde{c}r}}$	1.9845	0.4774	0.6737	0.5644	[0.9954, 1.6537]	2.1496	0.4901	0.8080	0.6852	[1.1133, 1.8389]
	$\beta_{L_{\tilde{c}r}}$	3.8415	0.1576	0.8556	0.8415	[3.1612, 3.9000]	3.5760	0.1355	0.5912	0.5760	[3.1142, 3.5203]
15 ($e = 20$)	$\alpha_{U_{\tilde{c}r}}$	1.1879	0.2288	0.3836	0.3165	[0.6040, 1.0886]	1.1112	0.2113	0.4400	0.3888	[0.5552, 1.0288]
	$\beta_{U_{\tilde{c}r}}$	3.9000	0.0000	0.9000	0.9000	[3.9000, 3.9000]	3.6494	0.0656	0.6526	0.6494	[3.5137, 3.6185]
	$\alpha_{L_{\tilde{c}r}}$	2.1724	0.4335	0.7941	0.7258	[0.9662, 2.0057]	2.3158	0.4476	0.9251	0.8577	[1.0811, 2.1272]
	$\beta_{L_{\tilde{c}r}}$	3.8722	0.0888	0.8765	0.8722	[3.5255, 3.9000]	3.6487	0.0845	0.6539	0.6487	[3.3942, 3.6447]
16 ($e = 7$)	$\alpha_{U_{\tilde{c}r}}$	1.0164	0.2001	0.5169	0.4836	[0.8168, 0.8854]	0.9662	0.1865	0.5603	0.5338	[0.7788, 0.8432]
	$\beta_{U_{\tilde{c}r}}$	3.9000	0.0000	0.9000	0.9000	[3.9000, 3.9000]	3.7045	0.0261	0.7049	0.7045	[3.6551, 3.7044]
	$\alpha_{L_{\tilde{c}r}}$	2.1779	0.4852	0.8098	0.6874	[1.4716, 1.8571]	2.3122	0.4832	0.9242	0.8122	[1.6181, 1.9714]
	$\beta_{L_{\tilde{c}r}}$	3.9000	0.0000	0.9000	0.9000	[3.9000, 3.9000]	3.7019	0.0549	0.7037	0.7019	[3.6057, 3.6812]

Table 3. Simulation results for the Log-Logistic current-record model when $\alpha = 2$ and $\beta = 5$.

		MLE					BE				
p	Parameter	Mean	SD	RMSE	MAD	95% CI	Mean	SD	RMSE	MAD	95% BCI
3 ($e = 3$)	$\alpha_{U_{\tilde{c}r}}$	2.4952	1.2518	1.1357	0.7919	[1.6311, 1.7775]	2.2885	0.9806	0.8510	0.6526	[1.6029, 1.7269]
	$\beta_{U_{\tilde{c}r}}$	4.1164	2.2363	2.0285	1.8836	[2.0644, 2.9245]	3.4150	1.4011	1.9547	1.5850	[1.9646, 2.7421]
	$\alpha_{L_{\tilde{c}r}}$	2.3267	1.3826	1.1752	0.9448	[1.3416, 1.5365]	2.2480	0.7096	0.6303	0.5087	[1.6090, 1.8662]
	$\beta_{L_{\tilde{c}r}}$	3.7107	2.4453	2.3767	2.2893	[1.9360, 2.3161]	3.1938	1.1554	2.0378	1.8062	[2.3135, 2.5396]
4 ($e = 10$)	$\alpha_{U_{\tilde{c}r}}$	2.1801	0.9452	0.9146	0.8276	[0.9557, 1.3042]	2.0618	0.6981	0.6651	0.5949	[1.0307, 1.4856]
	$\beta_{U_{\tilde{c}r}}$	3.7252	2.0841	2.3525	2.1748	[1.5182, 2.1194]	3.2936	1.2971	2.1038	1.7064	[1.4289, 2.3562]
	$\alpha_{L_{\tilde{c}r}}$	1.8790	0.9378	0.8979	0.7843	[0.8614, 1.1696]	1.9608	0.7647	0.7265	0.6508	[0.9974, 1.3372]
	$\beta_{L_{\tilde{c}r}}$	5.1683	1.9230	1.8321	1.7128	[1.8237, 3.5309]	4.1202	1.1305	1.3872	0.9022	[1.9296, 3.3201]
5 ($e = 38$)	$\alpha_{U_{\tilde{c}r}}$	2.2633	0.8733	0.9010	0.7011	[1.1529, 1.6582]	2.1176	0.6956	0.6964	0.5450	[1.1619, 1.6858]
	$\beta_{U_{\tilde{c}r}}$	4.6492	1.7275	1.7404	1.5488	[1.6576, 3.0710]	4.0212	1.0989	1.4607	1.0991	[1.6934, 3.1094]
	$\alpha_{L_{\tilde{c}r}}$	2.0225	0.6903	0.6815	0.5583	[0.8926, 1.4052]	2.1731	0.6528	0.6670	0.5685	[1.0036, 1.5828]
	$\beta_{L_{\tilde{c}r}}$	4.4554	1.7129	1.7758	1.6560	[2.0920, 2.9379]	3.9335	1.0804	1.5080	1.2091	[2.2328, 2.9946]
6 ($e = 66$)	$\alpha_{U_{\tilde{c}r}}$	2.1670	0.7143	0.7283	0.5761	[1.0103, 1.5807]	2.0527	0.5966	0.5944	0.4781	[1.1697, 1.5862]
	$\beta_{U_{\tilde{c}r}}$	4.6053	1.4636	1.5052	1.3507	[2.0678, 3.3574]	4.1449	0.9715	1.2887	1.0516	[2.3034, 3.4295]
	$\alpha_{L_{\tilde{c}r}}$	1.9730	0.6916	0.6869	0.5230	[0.7832, 1.4502]	2.1097	0.6263	0.6311	0.4832	[0.8791, 1.6922]
	$\beta_{L_{\tilde{c}r}}$	4.9524	1.4506	1.4404	1.3198	[2.2258, 3.4896]	4.3157	0.8573	1.0918	0.8506	[2.4487, 3.5309]
7 ($e = 124$)	$\alpha_{U_{\tilde{c}r}}$	2.0805	0.6222	0.6249	0.4575	[1.0122, 1.6928]	1.9593	0.5329	0.5323	0.4101	[1.0292, 1.6361]
	$\beta_{U_{\tilde{c}r}}$	5.0262	1.2699	1.2650	1.0994	[2.4954, 4.0428]	4.4781	0.8265	0.9747	0.7503	[2.5519, 3.9063]
	$\alpha_{L_{\tilde{c}r}}$	1.9761	0.5258	0.5243	0.4124	[0.7224, 1.6326]	2.1183	0.4977	0.5097	0.3997	[0.7976, 1.7796]
	$\beta_{L_{\tilde{c}r}}$	5.1826	1.3595	1.3662	1.2327	[1.8653, 3.9612]	4.5873	0.8966	0.9837	0.7525	[1.9994, 3.9083]
8 ($e = 145$)	$\alpha_{U_{\tilde{c}r}}$	2.0875	0.5230	0.5285	0.3984	[1.1335, 1.7417]	1.9627	0.4604	0.4603	0.3510	[1.1222, 1.6647]
	$\beta_{U_{\tilde{c}r}}$	5.4222	1.1903	1.2591	1.1520	[2.7437, 4.2897]	4.8253	0.8070	0.8230	0.6725	[2.6704, 4.1588]
	$\alpha_{L_{\tilde{c}r}}$	2.0735	0.4790	0.4830	0.3571	[1.1745, 1.7573]	2.2247	0.4704	0.5198	0.3933	[1.2836, 1.9233]
	$\beta_{L_{\tilde{c}r}}$	5.5022	1.0900	1.1966	1.0718	[3.1566, 4.6071]	4.9258	0.7362	0.7374	0.6342	[3.1014, 4.3544]
9 ($e = 150$)	$\alpha_{U_{\tilde{c}r}}$	2.0419	0.4388	0.4393	0.3220	[1.2252, 1.7456]	1.9204	0.3890	0.3958	0.3094	[1.2364, 1.6665]
	$\beta_{U_{\tilde{c}r}}$	5.8338	0.9029	1.2268	1.1016	[2.5000, 5.2445]	5.2019	0.6379	0.6671	0.5530	[2.5790, 4.8552]
	$\alpha_{L_{\tilde{c}r}}$	2.1220	0.5109	0.5236	0.3783	[1.2057, 1.7965]	2.2672	0.4873	0.5544	0.3911	[1.3221, 1.9431]
	$\beta_{L_{\tilde{c}r}}$	5.7425	1.0570	1.2889	1.1869	[2.4319, 4.9439]	5.1247	0.7314	0.7396	0.6319	[2.6516, 4.6546]
10 ($e = 170$)	$\alpha_{U_{\tilde{c}r}}$	1.9152	0.3449	0.3542	0.2850	[1.0762, 1.6484]	1.8097	0.3073	0.3606	0.2890	[1.0575, 1.5685]
	$\beta_{U_{\tilde{c}r}}$	5.9216	0.9077	1.2917	1.1883	[2.7888, 5.4055]	5.3381	0.6658	0.7450	0.6611	[2.7783, 5.0317]
	$\alpha_{L_{\tilde{c}r}}$	2.1059	0.3890	0.4021	0.3228	[1.1742, 1.8143]	2.2497	0.3986	0.4694	0.3763	[1.2574, 1.9749]
	$\beta_{L_{\tilde{c}r}}$	5.9517	0.8572	1.2791	1.1748	[2.5647, 5.6197]	5.3694	0.6439	0.7407	0.6403	[2.6118, 5.1372]
11 ($e = 103$)	$\alpha_{U_{\tilde{c}r}}$	1.9401	0.4337	0.4358	0.2986	[1.1231, 1.6801]	1.8332	0.3967	0.4286	0.3223	[1.1099, 1.6012]
	$\beta_{U_{\tilde{c}r}}$	6.2147	0.5917	1.3499	1.2861	[3.4859, 6.4483]	5.6332	0.4618	0.7824	0.7271	[3.3621, 5.5004]
	$\alpha_{L_{\tilde{c}r}}$	2.2354	0.4700	0.5236	0.3839	[0.8901, 1.9640]	2.3796	0.4726	0.6044	0.4704	[1.0039, 2.1157]
	$\beta_{L_{\tilde{c}r}}$	6.0752	0.7036	1.2831	1.2042	[3.9198, 5.9233]	5.5005	0.5184	0.7188	0.6570	[3.9204, 5.3367]
12 ($e = 83$)	$\alpha_{U_{\tilde{c}r}}$	1.8235	0.2618	0.3144	0.2584	[1.2768, 1.6466]	1.7265	0.2440	0.3655	0.3137	[1.1875, 1.5670]
	$\beta_{U_{\tilde{c}r}}$	6.2305	0.6016	1.3681	1.2996	[3.3604, 6.3988]	5.6788	0.4744	0.8265	0.7674	[3.3071, 5.5968]
	$\alpha_{L_{\tilde{c}r}}$	2.2050	0.2809	0.3464	0.2746	[1.6190, 2.0343]	2.3397	0.2881	0.4443	0.3636	[1.7556, 2.1447]
	$\beta_{L_{\tilde{c}r}}$	6.2048	0.6694	1.3763	1.3158	[2.8244, 6.4042]	5.6999	0.5435	0.8842	0.8275	[2.8302, 5.6140]
13 ($e = 59$)	$\alpha_{U_{\tilde{c}r}}$	1.7845	0.2981	0.3658	0.3111	[1.3056, 1.5698]	1.7012	0.2819	0.4092	0.3620	[1.2604, 1.4931]
	$\beta_{U_{\tilde{c}r}}$	6.2763	0.4423	1.3495	1.2783	[4.9414, 6.4003]	5.8067	0.3628	0.8832	0.8179	[4.8079, 5.6355]
	$\alpha_{L_{\tilde{c}r}}$	2.2212	0.3502	0.4117	0.3352	[1.4429, 1.9811]	2.3591	0.3698	0.5132	0.4224	[1.5311, 2.1168]
	$\beta_{L_{\tilde{c}r}}$	6.3618	0.3216	1.3987	1.3642	[4.9300, 6.5000]	5.8414	0.2907	0.8894	0.8470	[4.8345, 5.7290]
14 ($e = 22$)	$\alpha_{U_{\tilde{c}r}}$	1.6975	0.2089	0.3649	0.3207	[1.3426, 1.5443]	1.6168	0.2036	0.4317	0.3874	[1.2663, 1.4525]
	$\beta_{U_{\tilde{c}r}}$	6.4581	0.1521	1.4656	1.4581	[5.8161, 6.5000]	5.9658	0.1826	0.9821	0.9658	[5.4853, 5.8613]
	$\alpha_{L_{\tilde{c}r}}$	2.3196	0.2807	0.4211	0.3305	[1.8800, 2.0791]	2.4490	0.2805	0.5260	0.4490	[2.0287, 2.2071]
	$\beta_{L_{\tilde{c}r}}$	6.3826	0.3513	1.4245	1.3826	[5.0111, 6.5000]	5.9016	0.3056	0.9497	0.9158	[4.8432, 5.7698]
15 ($e = 18$)	$\alpha_{U_{\tilde{c}r}}$	1.7489	0.2835	0.3728	0.3193	[1.3615, 1.5526]	1.6741	0.2694	0.4180	0.3624	[1.2831, 1.4973]
	$\beta_{U_{\tilde{c}r}}$	6.4399	0.2548	1.4611	1.4399	[5.4189, 6.5000]	6.0476	0.2322	1.0716	1.0476	[5.1981, 6.0451]
	$\alpha_{L_{\tilde{c}r}}$	2.5209	0.3167	0.6051	0.5209	[2.0651, 2.3049]	2.6410	0.3535	0.7272	0.6410	[2.1829, 2.3990]
	$\beta_{L_{\tilde{c}r}}$	6.3880	0.3225	1.4230	1.3880	[5.4126, 6.5000]	6.0043	0.2787	1.0401	1.0043	[5.2412, 5.9704]
16 ($e = 9$)	$\alpha_{U_{\tilde{c}r}}$	1.5594	0.2926	0.5083	0.4406	[1.2756, 1.3927]	1.5004	0.2758	0.5537	0.4996	[1.2331, 1.3458]
	$\beta_{U_{\tilde{c}r}}$	6.5000	0.0000	1.5000	1.5000	[6.5000, 6.5000]	6.1738	0.0184	1.1739	1.1738	[6.1529, 6.1653]
	$\alpha_{L_{\tilde{c}r}}$	2.5801	0.5456	0.7482	0.6240	[1.9121, 2.3463]	2.7081	0.5636	0.8600	0.7081	[2.0131, 2.4589]
	$\beta_{L_{\tilde{c}r}}$	6.3312	0.3376	1.3629	1.3312	[5.8248, 6.3312]	5.9344	0.2714	0.9635	0.9344	[5.5452, 5.8657]

6.1. Discussion of the simulation results

Tables 1–3 summarize the Monte Carlo results for the proposed maximum likelihood (MLE) and Bayesian (BE) estimators under different combinations of the Log-Logistic parameters. Overall, both estimation procedures perform satisfactorily and exhibit clear improvements as the number of current records increases. Since larger values of p contain more record information, the estimators become increasingly stable and their sampling variability decreases.

For both upper and lower current records, the standard deviations, RMSEs, and MADs generally decrease as the current-record size increases. This behavior demonstrates the consistency of the proposed estimators, since additional record observations provide more information about the unknown parameters. The improvement is particularly evident for the scale parameter α, whose estimates become progressively more concentrated around the true parameter values as p increases.

Comparing the two estimation methods shows that the Bayesian estimators consistently produce smaller standard deviations than the corresponding maximum likelihood estimators in almost all scenarios. The Bayesian approach also yields smaller RMSE and MAD values in most cases, especially when the number of available current records is relatively small. This improvement is expected because the incorporation of prior information stabilizes the estimation process and reduces sampling variability.

For the shape parameter β, both estimation methods gradually approach the true parameter values as the number of current records increases. Although the MLE occasionally exhibits larger variability for small values of p, the Bayesian estimates remain more stable throughout the simulation study. As expected, the differences between the two methods become smaller as the record size increases, indicating that both estimators are asymptotically reliable when sufficient current-record information is available.

A comparison of Tables 1–3 further indicates that increasing the true parameter values does not alter the overall performance of the proposed procedures. The same convergence patterns are observed for all three parameter combinations, confirming that the proposed estimation methods are robust across different shapes and scales of the Log-Logistic distribution.

Overall, the simulation study demonstrates that the newly derived gamma-based current-record likelihood functions provide accurate and reliable inference for the Log-Logistic distribution. Both the maximum-likelihood and Bayesian approaches perform well, with the Bayesian procedure generally offering greater numerical stability and improved finite-sample accuracy. These findings support the practical applicability of the proposed methods for analyzing environmental current-record data, particularly in situations where only record observations are available. ‘‘‘

7. Bayesian Prediction (BP)

In this subsection, Bayesian prediction of future current records is developed using the posterior predictive approach based on the proposed current-record distributions. The predictive distribution is obtained by integrating the conditional distribution of a future current record with respect to the posterior distribution of the unknown parameters derived in Section 5. Since the posterior densities involve the regularized incomplete gamma function, closed-form Bayesian predictors are not available, and Monte Carlo simulation is employed for numerical implementation.

Bayesian prediction for upper current records: Let $U_{\tilde{cr}}^{p+s}$ denote the $(p+q)$-th upper current record, given the observed upper current records

$$\underline{U_{\tilde{cr}}} = \left(U_{\tilde{cr}}^{1}, U_{\tilde{cr}}^{2}, \ldots, U_{\tilde{cr}}^{p}\right).$$

The posterior predictive density is defined by

$$f^{BP}_{U_{\tilde{cr}}^{p+q}|\underline{U_{\tilde{cr}}}}(u) = \int f_{U_{\tilde{cr}}^{p+q}|U_{\tilde{cr}}^{p}}(u \mid u_p, \alpha, \beta)\, \pi(\alpha, \beta \mid \underline{U_{\tilde{cr}}})\, d\alpha\, d\beta, \tag{25}$$

where $f_{U_{\tilde{cr}}^{p+q}|U_{\tilde{cr}}^{p}}(\cdot)$ denotes the conditional density of the future upper current record and $\pi(\alpha, \beta \mid \underline{U_{\tilde{cr}}})$ is the posterior distribution obtained in Section 5.

Substituting the conditional density of the proposed upper current-record model yields

$$f^{BP}_{U_{\tilde{cr}}^{p+q}|\underline{U_{\tilde{cr}}}}(u) \propto \int f_{U_{\tilde{cr}}^{p+q}|U_{\tilde{cr}}^{p}}(u \mid u_p, \alpha, \beta) \times \pi(\alpha, \beta \mid \underline{U_{\tilde{cr}}})\, d\alpha\, d\beta, \qquad u \geq u_p. \tag{26}$$

Under the squared error loss function, the Bayesian point predictor is

$$\widehat{U_{\tilde{cr}}^{p+q}}^{BP} = E\big(U_{\tilde{cr}}^{p+q} \mid \underline{U_{\tilde{cr}}}\big) = \int_{u_p}^{1} u f^{BP}_{U_{\tilde{cr}}^{p+q}|\underline{U_{\tilde{cr}}}}(u) du. \tag{27}$$

Since the posterior predictive density has no closed-form expression, the Bayesian predictor is approximated using Monte Carlo simulation,

$$\widehat{U_{\tilde{cr}}^{p+q}}^{BP} \approx \frac{1}{T}\sum_{t=1}^{T} U_{\tilde{cr}}^{p+q,(t)},$$

where $\{U_{\tilde{cr}}^{p+q,(t)}\}_{t=1}^{T}$ are generated from the posterior predictive distribution. A $100(1-\gamma)\%$ Bayesian prediction interval is obtained from the posterior predictive distribution,

$$P\left(L_\gamma \leq U_{\tilde{cr}}^{p+q} \leq U_\gamma \mid \underline{U_{\tilde{cr}}}\right) = 1 - \gamma,$$

whose limits are estimated using the empirical posterior predictive quantiles,

$$(L_\gamma, U_\gamma) = \left(Q_{\gamma/2}, Q_{1-\gamma/2}\right).$$

Bayesian prediction for lower current records: Exactly the same work can be done as the upper current record but using relevant formulas.

The Bayesian predictive approach naturally incorporates parameter uncertainty through the posterior distribution while preserving the stochastic structure of the proposed current-record model. Consequently, both the Bayesian point predictors and prediction intervals fully reflect the uncertainty associated with future current records. Since the predictive integrals involve the regularized incomplete gamma function and do not admit closed-form solutions, posterior predictive quantities are evaluated numerically using the Metropolis–Hastings algorithm described in Section 5.

8. Real Saudi Environmental Data

The real-data analysis presented in this section is intended primarily as an illustrative application of the proposed current-record methodology rather than as a comprehensive climatological study of Riyadh. The 31 daily atmospheric-pressure observations are used to demonstrate, in a transparent and manageable setting, how the upper and lower current records are extracted, how the unknown Log-Logistic parameters are estimated from these records, and, most importantly, how the proposed prediction procedures can be used to obtain future upper and lower current records and their associated prediction intervals. Accordingly, the purpose of this application is to verify the practical implementability of the proposed statistical methodology rather than to draw conclusions regarding long-term climate change or seasonal atmospheric-pressure behavior.

A substantially longer observational period would naturally be preferable for climatological or seasonal inference. Such an extension would also generally produce a richer set of current-record observations and consequently require a considerably larger empirical presentation, including additional record tables, estimation results, and prediction outputs. Since the principal contribution of the present study is the development of the new Log-Logistic current-record framework and its associated estimation and prediction procedures, the present dataset was retained as a concise empirical illustration of the methodology. Future applications using annual or multi-year atmospheric datasets would provide an important extension for investigating seasonal and long-term pressure behavior.

To illustrate the practical applicability of the proposed methodology, a real environmental dataset from Saudi Arabia is analyzed. The dataset consists of daily average atmospheric pressure measurements recorded in Riyadh over the period from October 27, 2025, to November 26, 2025, and is publicly available at https://doi.org/10.6084/m9.figshare.30720569. Before applying the proposed current record methodology, the underlying distribution of the observations was investigated.

1015.7, 1015.5, 1014.35, 1013.4, 1015.15, 1016.7, 1018.1, 1018.75, 1018.15, 1017.55, 1016.8, 1017.4, 1018.85, 1019.1, 1017.9, 1017.3, 1018.45, 1020.05, 1018, 1016.15, 1019.35, 1021.7, 1021.5, 1021.05, 1022.55, 1023.15, 1022.85, 1021.75, 1020.4, 1020.1, 1019.2

Table 4. Comparison of candidate distributions for the Riyadh atmospheric-pressure data.

Distribution	Log-likelihood	AIC	BIC	KS	KS p-value
Log-Logistic	-72.9047	149.8095	152.6774	0.0745	0.9903
Weibull	-73.6112	151.2224	154.0903	0.1234	0.6872
GEV	-71.7003	149.4007	153.7026	0.0751	0.9893

To further assess the suitability of the Log-Logistic distribution for the Riyadh atmospheric-pressure data, its fit was compared with the Weibull and Generalized Extreme Value (GEV) distributions, which provide relevant alternative models for positive environmental observations and extreme-value behavior. The comparison was performed using the maximized log-likelihood, Akaike information criterion (AIC), Bayesian information criterion (BIC), and Kolmogorov–Smirnov (KS) goodness-of-fit statistic, as reported in Table 4.

The results indicate that the Log-Logistic distribution provides a highly competitive fit to the observed pressure data. Its AIC and BIC values are comparable with those obtained from the competing models, while its KS statistic of 0.0745 and corresponding p-value of 0.9903 indicate excellent agreement between the fitted distribution and the empirical observations. In particular, the Log-Logistic model produces a substantially smaller KS statistic than the Weibull model, while its goodness-of-fit performance is very close to that of the GEV model. These findings, together with the Anderson–Darling and Cram'er–von Mises results reported above and the graphical goodness-of-fit diagnostics, provide sufficient empirical support for using the Log-Logistic distribution as the parent model in the illustrative current-record analysis. The purpose of this comparison is not to claim universal superiority of the Log-Logistic distribution, but rather to demonstrate that it provides an adequate and competitive representation of the present atmospheric-pressure dataset for illustrating the proposed current-record methodology. The suitability of the log-logistic distribution for modeling the pressure data was assessed using maximum likelihood estimation and several goodness-of-fit tests. The maximum likelihood estimates of the scale and shape parameters were $\hat{\alpha} = 1018.5931$ and $\hat{\beta} = 702.3362$, respectively. The Kolmogorov–Smirnov test produced a test statistic of $D = 0.074506$ with a p-value of 0.9903, while the Anderson–Darling test yielded $A = 0.17479$ with a p-value of 0.9959. Similarly, the Cramér–von Mises test resulted in $\omega^2 = 0.021119$ with a p-value of 0.9964. Since the p-values of all three goodness-of-fit tests are substantially greater than the significance level of $\alpha = 0.05$, the null hypothesis that the data follow a log-logistic distribution cannot be rejected. Furthermore, the diagnostic plots, including the histogram with the fitted probability density function, the empirical and fitted cumulative distribution functions, the Q–Q plot, the P–P plot, and the kernel density plot in Figure 4, all demonstrate excellent agreement between the observed data and the fitted log-logistic model. Therefore, the log-logistic distribution provides an excellent representation of the pressure data and is appropriate for subsequent statistical analysis.

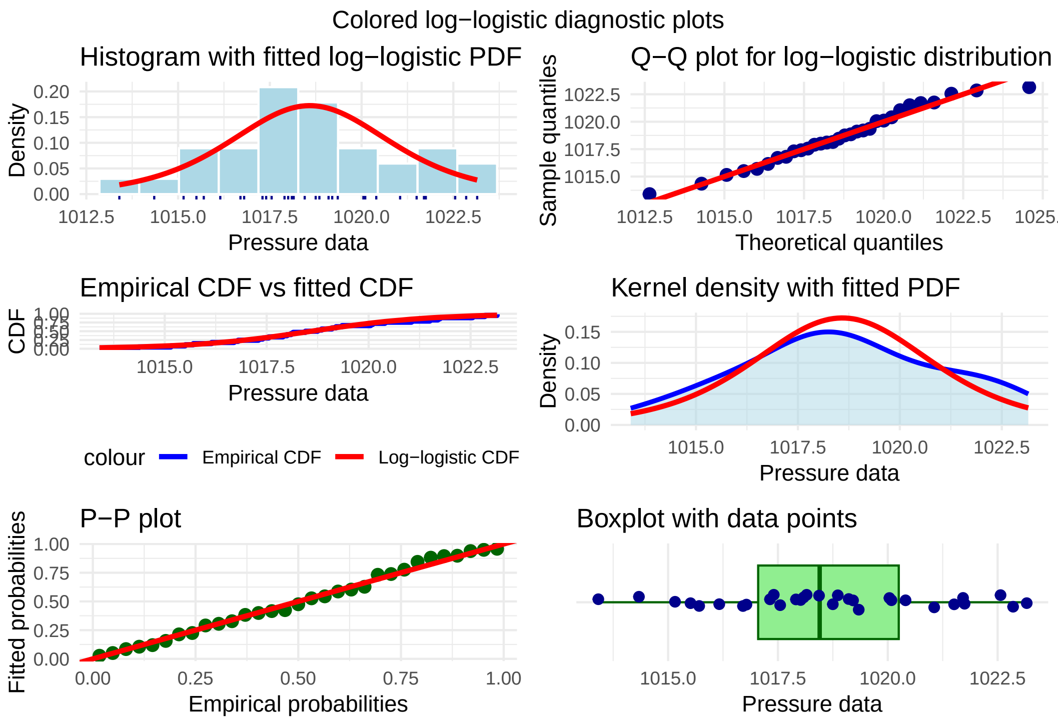

Figure 4. Goodness-of-fit diagnostics for the fitted Log-Logistic distribution with $\hat{\alpha} = 1018.5931$ and $\hat{\beta} = 702.3362$.

Based on these observations, the corresponding upper and lower current records were extracted and subsequently used to illustrate the proposed inferential procedures and prediction methods developed in this paper and recorded in Table 5.

Table 5. Upper current record $U^p_{\tilde{c}r}$, lower current record $L^p_{\tilde{c}r}$, and current record range $R^p_{\tilde{c}r}$ for the Riyadh atmospheric pressure data.

Record No. (p)	$U^p_{\tilde{c}r}$	$L^p_{\tilde{c}r}$	$R^p_{\tilde{c}r}$
1	1015.70	1015.70	0.00
2	1015.70	1015.50	0.20
3	1015.70	1014.35	1.35
4	1015.70	1013.40	2.30
5	1016.70	1013.40	3.30
6	1018.10	1013.40	4.70
7	1018.75	1013.40	5.35
8	1018.85	1013.40	5.45
9	1019.10	1013.40	5.70
10	1020.05	1013.40	6.65
11	1021.70	1013.40	8.30
12	1022.55	1013.40	9.15
13	1023.15	1013.40	9.75

Now, using equations from Section 5, the following results stored in Table 6 are the MLE and BE of the Log-Logistic current records' parameters, along with their 95% bootstrap confidence intervals.

Table 6. MLE and BE of the Log-Logistic parameters based on upper and lower current records.

Record	Method	$\hat{\alpha}$ (95% interval)	$\hat{\beta}$ (95% interval)
Upper	MLE	1014.7580 (1013.8463, 1015.6704)	1155.6293 (879.8684, 1517.8169)
Lower	MLE	1015.4028 (1015.0170, 1015.7886)	2702.9915 (2092.2656, 3491.9865)
Upper	Bayesian	1014.4810 (1013.1460, 1015.4526)	1080.9872 (789.0285, 1426.2317)
Lower	Bayesian	1015.6834 (1015.1664, 1016.5600)	2275.8464 (1523.3295, 2937.4336)

After that, equations from Section 7 are applied to get the prediction of the next 3 future upper, lower, and current ranges with the values writed in Table 7.

Table 7. Point predictions and 95% prediction intervals for future Log-Logistic current records under BE and MLE.

q	Bayesian Estimation (BE)			Maximum Likelihood Estimation (MLE)		
	$\widehat{U}_{\tilde{c}r}^{14+q}$	$\widehat{L}_{\tilde{c}r}^{14+q}$	$\widehat{R}_{\tilde{c}r}^{14+q}$	$\widehat{U}_{\tilde{c}r}^{14+q}$	$\widehat{L}_{\tilde{c}r}^{14+q}$	$\widehat{R}_{\tilde{c}r}^{14+q}$
1	1024.1020 (1023.1735, 1026.6890)	1012.9410 (1011.6716, 1013.3889)	11.1610 (9.9078, 13.9788)	1024.0450 (1023.1720, 1026.4260)	1013.0214 (1011.9815, 1013.3903)	11.0236 (9.8885, 13.5535)
2	1025.0874 (1023.3661, 1028.7208)	1012.4901 (1010.7885, 1013.2915)	12.5972 (10.4515, 16.4278)	1024.9157 (1023.3656, 1028.0850)	1012.6493 (1011.3089, 1013.3096)	12.2664 (10.3876, 15.6134)
3	1026.0616 (1023.7207, 1030.4059)	1012.0320 (1009.9124, 1013.1253)	14.0295 (11.1853, 18.7483)	1025.8112 (1023.6976, 1029.5928)	1012.2745 (1010.6947, 1013.1648)	13.5366 (11.0420, 17.4879)

Tables 5 and 6 present the predicted future upper and lower current atmospheric-pressure records in Riyadh obtained using the maximum likelihood and Bayesian approaches, respectively. Both methods produce highly consistent prediction results, indicating the stability and reliability of the proposed Log-Logistic current-record model. The predicted future upper current records increase gradually with the prediction horizon, from approximately 1024.05–1024.10 hPa for the first future record to about 1025.81–1026.06 hPa for the third future record. This behavior is expected because upper current records represent successive record-breaking high pressure values, and each future record must exceed the previous maximum observed pressure of 1023.15 hPa.

Conversely, the predicted lower current records decrease slightly as the prediction horizon increases, from approximately 1013.02 hPa (MLE) and 1012.94 hPa (BE) for the first future record to approximately 1012.27 hPa (MLE) and 1012.03 hPa (BE) for the third future record. Since lower current records correspond to new minimum atmospheric-pressure observations, this gradual decrease is consistent with the theoretical properties of current records.

The predicted current-record range also increases with the prediction horizon, from approximately 11 hPa for the first future record to approximately 13.5–14.0 hPa for the third future record. This behavior reflects the structure of the fitted current-record model, under which successive predicted upper records tend to increase while successive lower records tend to decrease. These predictions should therefore be interpreted as model-based illustrations conditional on the observed dataset and the fitted Log-Logistic model, rather than as evidence of a long-term change in Riyadh atmospheric-pressure variability.

It should be noted that these predictions are conditional on the fitted Log-Logistic current-record model and are intended to illustrate the predictive implementation of the proposed methodology. Since the empirical application is based on a relatively short observational period, the resulting predictions should not be interpreted as long-term climatological forecasts. Validation using longer time series, different seasons, and additional locations would provide a useful extension for assessing the predictive performance of the proposed current-record framework under broader environmental conditions.

A comparison of the two estimation methods shows only minor differences in both the point predictions and the associated prediction intervals. The Bayesian predictions are slightly more conservative for the lower records and slightly larger for the upper records, resulting in marginally wider prediction intervals. This behavior reflects the incorporation of parameter uncertainty through the posterior distribution. Nevertheless, the close agreement between the Bayesian and maximum likelihood predictions provides strong evidence that the proposed prediction methodology is robust and yields reliable forecasts of future atmospheric-pressure extremes in Riyadh.

8.1. MCMC convergence diagnostic

For the Bayesian computation, three independent Metropolis–Hastings chains with dispersed initial values were employed to assess convergence. Each chain was run for 50,000 iterations, with the first 10,000 iterations discarded as burn-in. Every fifth subsequent draw was retained, resulting in 8,000 posterior draws per chain. Convergence was assessed using the Gelman–Rubin potential scale reduction factor ($\hat{R}$), effective sample size (ESS), trace plots, and autocorrelation functions (ACFs). The corresponding diagnostic results are reported in Table 8.

Table 8. MCMC convergence diagnostics for the Bayesian estimates based on the Riyadh atmospheric-pressure current records.

Record type	Parameter	$\hat{R}$	ESS	Acceptance rate
Upper	α	1.0055	2202.7	0.6362
Upper	β	1.0048	1683.8	0.6362
Lower	α	1.0007	1917.6	0.4540
Lower	β	1.0016	1319.7	0.4540

The convergence diagnostics provide strong evidence of satisfactory MCMC convergence. For the upper current records, the $\hat{R}$ values are 1.0055 and 1.0048 for α and β, respectively, whereas the corresponding values for the lower current records are 1.0007 and 1.0016. Thus, all $\hat{R}$ values are very close to one, indicating good agreement among the three independent chains. The effective sample sizes range from 1319.7 to 2202.7, providing an adequate number of effectively independent posterior draws for inference. The mean Metropolis–Hastings acceptance rates are 0.6362 and 0.4540 for the upper and lower current-record analyses, respectively. Overall, these diagnostics support the stability and reliability of the posterior estimates used in the subsequent Bayesian analysis.

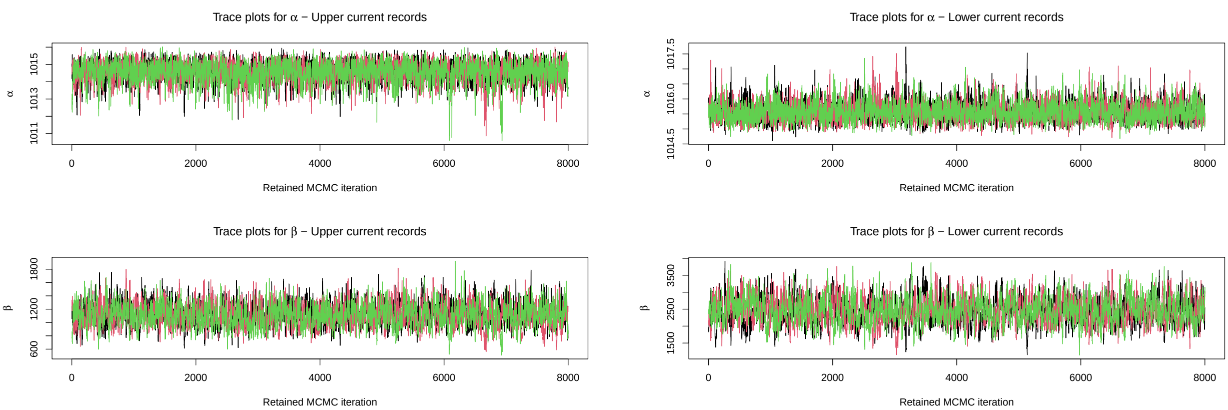

Figure 5. Trace plots of the three independent MCMC chains for the Log-Logistic parameters α and β based on the upper and lower current records.

The trace plots in Figure 5 show that the three independent chains fluctuate around common stable levels without persistent trends, which, together with the $\hat{R}$ and ESS results, provides further evidence of satisfactory MCMC convergence.

8.2. *Prior-sensitivity analysis*

To examine the robustness of the Bayesian estimates to the choice of prior, a sensitivity analysis was conducted using three independent Gamma prior specifications for the Log-Logistic parameters α and β. The three prior settings were constructed to preserve approximately the same prior means while varying the degree of prior concentration. In particular, the prior means were centered approximately at $E(\alpha) = 1018$ and $E(\beta) = 1000$, whereas the prior variances decreased progressively from Prior I to Prior III. This construction makes it possible to assess whether changes in the amount of prior information materially affect the posterior estimates.

For each prior specification, posterior samples were generated using the Metropolis–Hastings algorithm for both upper and lower current records. Posterior means, 95% Bayesian credible intervals, and acceptance rates are reported in Table 9.

Table 9. Prior-sensitivity analysis of the Bayesian estimates for the Riyadh atmospheric-pressure current records.

Prior	Record type	$\hat{\alpha}^{BE}$ (95% BCI)	$\hat{\beta}^{BE}$ (95% BCI)	Acceptance rate
Prior I	Upper	1014.6155 (1013.3741, 1015.5186)	1135.5151 (817.6532, 1486.0550)	0.6335
Prior I	Lower	1015.5218 (1015.0346, 1016.1716)	2547.5772 (1787.7389, 3368.4238)	0.4451
Prior II	Upper	1014.5220 (1013.0743, 1015.4953)	1103.3398 (782.1514, 1462.7886)	0.6381
Prior II	Lower	1015.5957 (1015.0654, 1016.3309)	2417.9933 (1696.9648, 3227.7548)	0.4542
Prior III	Upper	1014.5224 (1013.2390, 1015.4511)	1098.8708 (789.3495, 1431.1985)	0.6319
Prior III	Lower	1015.6779 (1015.1367, 1016.4381)	2291.2862 (1639.0119, 3027.7246)	0.4717

The sensitivity results indicate that the posterior estimates of the scale parameter α are highly stable under the three prior specifications. For the upper current records, the posterior mean of α ranges only from 1014.5220 to 1014.6155, while for the lower current records, it ranges from 1015.5218 to 1015.6779. The corresponding relative variations are approximately 0.009% and 0.015%, respectively. Thus, the posterior inference for α is practically insensitive to the selected Gamma prior specification.

The posterior estimates of the shape parameter β exhibit somewhat greater variation. For the upper current records, the posterior means range from 1098.8708 to 1135.5151, corresponding to a relative variation of approximately 3.29%. For the lower-current records, the posterior means range from 2291.2862 to 2547.5772, with a relative variation of approximately 10.60%. Nevertheless, the corresponding 95% Bayesian credible intervals overlap considerably under all three prior specifications. Hence, although the lower-record estimate of β shows moderate sensitivity to the strength of the prior, the overall inferential conclusions remain qualitatively unchanged.

The Metropolis–Hastings acceptance rates range from 0.4451 to 0.6381 across all prior specifications and record types, indicating satisfactory movement of the Markov chains. Overall, the sensitivity analysis confirms that the principal Bayesian conclusions, particularly those concerning the scale parameter and the general behavior of the current-record model, are not driven by a single prior specification.

9. Conclusion

This paper developed a comprehensive statistical framework for analyzing current records under the Log-Logistic distribution. New closed-form probability density and cumulative distribution functions were derived for the upper and lower current records by utilizing recently established general current-record formulas. Based on these distributions, explicit joint and conditional densities, moment expressions, entropy and extropy, maximum-likelihood estimation procedures, Bayesian estimation methods, and posterior predictive techniques were developed. Since the resulting likelihood equations involve the regularized incomplete gamma function, efficient numerical optimization and Markov Chain Monte Carlo algorithms were employed to estimate the unknown parameters and obtain Bayesian predictions.

The proposed estimation procedures were evaluated through an extensive Monte Carlo simulation study across different parameter settings and sample sizes. The simulation results demonstrated that the accuracy of both maximum likelihood and Bayesian estimators improves as the number of available current records increases, with reductions in standard deviation, root mean square error, and mean absolute deviation. Overall, the Bayesian approach generally produced more stable estimates and slightly better predictive performance by accounting for parameter uncertainty.

The methodology was further illustrated using daily atmospheric-pressure observations from Riyadh, Saudi Arabia. Goodness-of-fit analyses confirmed that the Log-Logistic distribution provides an excellent representation of the observed pressure data. The estimated model was then used to predict future upper and lower current pressure records together with their prediction intervals. The prediction results indicate a gradual increase in future record-high atmospheric pressures and a slight decrease in future record-low pressures, leading to an increasing current-record range over successive prediction horizons. The close agreement between the maximum likelihood and Bayesian predictions further demonstrates the robustness and reliability of the proposed methodology.

The proposed current-record framework provides a practical statistical tool for modeling and predicting sequential atmospheric-pressure extremes when record observations are of primary interest. The Riyadh application should be regarded as an illustrative demonstration of the proposed estimation and prediction procedures rather than as an assessment of long-term climate change. In particular, the analysis demonstrates how observed pressure measurements can be transformed into upper and lower current records, which can then be used to estimate model parameters and predict future record values, along with their associated uncertainty. Applications to longer annual or multi-year datasets would be valuable for investigating seasonal behavior and long-term meteorological variability. The proposed methodology may also be extended to other environmental variables, including temperature, rainfall, wind speed, humidity, and air-quality measurements, as well as to applications in hydrology, engineering, reliability, finance, and other fields involving sequential extreme observations.

Acknowledgment

The authors extend their appreciation to Prince Sattam bin Abdulaziz University for funding this research work through the project number (PSAU/2026/02/44941).

Competing Interest

There are no relevant financial or non-financial competing interests to report.

References

[1] R. A. Aldallal. “Bayesian estimation and prediction of Weibull current records with application to Saudi industrial data”. In: *AIMS Mathematics* 11.2 (2026), pp. 4369–4394.

[2] R. A. Aldallal. “Best linear unbiased estimation and prediction of record values based on Kumaraswamy distributed data”. In: *Statistics, Optimization & Information Computing* 10.4 (2022), pp. 1250–1266.

[3] R. A. Aldallal. “Current record range of Laplace distributed data with application on Saudi Arabia industrial data”. In: *Journal of Statistics Applications and Probability* 14 (2025), pp. 723–729.

[4] R. A. Aldallal. “Fréchet Current Records: Bayesian and Non-Bayesian Estimation and Prediction with Application to Saudi Industrial Data”. In: *Letters in Biomathematics* 13.1 (2026), pp. 194–213.

[5] R. A. Aldallal. “Moment generating function of current records based on generalized exponential distribution with some recurrence relations”. In: *European Journal of Pure and Applied Mathematics* 16.1 (2023), pp. 97–111.

[6] R. A. Aldallal. “Rayleigh current record distributed data: Estimation and prediction with application on Saudi Arabia industrial data”. In: *Journal of Statistical Theory and Applications* 25.1 (2026), pp. 1–21.

[7] R. A. Aldallal and M. R. Alseedy. “Bayesian Prediction of Future Network Latency Times Under Two-Parameter Exponential Current Records”. In: *Mathematical and Computational Applications (MCA)* 31.4 (2026), p. 130.

[8] R. A. Aldallal and H. M. Barakat. “A comprehensive review: Current record values and their applications”. In: *Applied Mathematics and Information Sciences* 20.2 (2026), pp. 401–423.

[9] R. A. Aldallal and I. Sadok. “Bayesian Current Record Analysis for Mixed Rayleigh–Weibull Distributions with Application to Saudi Humidity Data”. In: *Statistics, Optimization & Information Computing* (2026).

[10] H. M. Barakat, E. M. Nigm, and R. A. Aldallal. “Current records and record range with some applications”. In: *Journal of the Korean Statistical Society* 43.2 (2014), pp. 263–273.

[11] H. M. Barakat, E. M. Nigm, and R. A. Aldallal. “Exact prediction intervals for future current records and record range from any continuous distribution”. In: *SORT* 38.2 (2014), pp. 251–270.

[12] A. M. Ghanem and Y. A. Alamri. “The impact of the Green Middle East Initiative on sustainable development in the Kingdom of Saudi Arabia”. In: *Journal of the Saudi Society of Agricultural Sciences* 22.1 (2023), pp. 35–46. DOI: 10.1016/j.jssas.2022.06.001.

[13] R. L. Houchens. “Record value theory and inference”. PhD thesis. University of California, Riverside, 1984.

[14] F. Lad, G. Sanfilippo, and G. Agro. “Extropy: Complementary dual of entropy”. In: *Statistical Science* (2015), pp. 40–58.

[15] M. F. McCabe et al. *Climate Futures Report: Saudi Arabia in a 3-Degrees Warmer World*. Tech. rep. Thuwal, Saudi Arabia: King Abdullah University of Science, Technology (KAUST), AEON Collective, and KAPSARC, 2023. DOI: 10.25781/KAUST-8XY63.

[16] A. K. Nassar. “Strategic energy transition in the Gulf Cooperation Council: Balancing economic, social, political, and environmental dynamics for sustainable development”. In: *International Journal of Green Energy* 22.8 (2025), pp. 1570–1586. DOI: 10.1080/15435075.2024.2435434.

[17] M. Z. Raqab. “Bounds on expectations of record range and record increment from distributions with bounded support”. In: *Journal of Inequalities in Pure and Applied Mathematics* 8.1 (2007).

[18] M. Z. Raqab. “Distribution-free prediction intervals for the future current record statistics”. In: *Statistical Papers* 50 (2009), pp. 429–439.

[19] M. Z. Raqab. “Inequalities for expected current record statistics”. In: *Communications in Statistics—Theory and Methods* 36.7 (2007), pp. 1367–1380.

[20] C. Shannon. “A mathematical theory of communication”. In: *The Bell System Technical Journal* 27.3 (1948), pp. 379–423.